Boundary Resonances in $S = 1/2$ Antiferromagnetic Chains under a Staggered Field

Shunsuke C. Furuya[1, 2] and Masaki Oshikawa[2]

[1] *Department of Physics, University of Tokyo, Hongo, Tokyo 113-0033, Japan*
[2] *Institute for Solid State Physics, University of Tokyo, Kashiwa 277-8581, Japan*

(Dated: November 30, 2012)

We develop a boundary field theory approach to electron spin resonance in open $S = 1/2$ Heisenberg antiferromagnetic chains with an effective staggered field. In terms of the sine Gordon effective field theory with boundaries, we point out the existence of boundary bound states of elementary excitations, and modification of the selection rules at the boundary. We argue that several "unknown modes" found in electron spin resonance experiments on $KCuGaF_6$ [I. Umegaki *et al.*, Phys. Rev. B **79**, 184401 (2009)] and Cu-PM [S. A. Zvyagin *et al.*, Phys. Rev. Lett. **93**, 027201 (2004)] can be understood as boundary resonances introduced by these effects.

PACS numbers: 76.30.-v, 11.10.Lm, 02.30.Ik, 75.10.Jm

Introduction. — Impurities often introduce new aspects in physics, Kondo effect being a notable example. In particular, impurity effects in strongly correlated systems are currently among central topics in condensed matter physics. Although the standard perturbation theory can fail, there are number of powerful theoretical approaches to strongly correlated systems, especially in one dimension. Impurity effects in gapless one-dimensional systems have been vigorously studied in terms of boundary conformal field theory. In contrast, impurity effects in gapped one-dimensional systems received much less attention, with the exception of the edge states in the $S = 1$ Haldane gap phase [1–3].

On the other hand, integrable models and field theories have been successfully applied to many gapped one-dimensional systems. In quantum magnetism, a field-induced gap in $S = 1/2$ Heisenberg antiferromagnetic (HAFM) chains is described in terms of a quantum sine Gordon field theory [4–6]; the one-dimensional Ising chain with critical transverse field and a weak longitudinal field realizes a quantum field theory with E_8 symmetry [7, 8]. Experimental studies indeed found elementary excitations predicted by these integrable field theories. Application of integrable field theories to impurity/boundary effects in gapped one-dimensional strongly correlated systems is an interesting but largely unexplored subject.

In this Letter, we present a theory of electron spin resonance (ESR) in $S = 1/2$ HAFM chains in a staggered field with boundaries, which may be realized by nonmagnetic impurities. The low-energy effective theory of the system is the quantum sine Gordon field theory with boundaries. In fact, this theory is integrable even in the presence of a boundary, and boundary bound states (BBS) of elementary excitations have been found in the exact solution [9–14]. The existence of BBS, and modification of the selection rules, imply extra resonances in addition to those in the bulk. ESR measurements on corresponding systems $KCuGaF_6$ [15] and $[\text{PM-Cu}(NO_3)_2(H_2O)_2]_n$ (PM denotes pyrimidine, abbreviated as Cu-PM) [16, 17] had found several resonances that could not be accounted for by the theory. We argue that several of those resonances can be successfully identified in terms of the boundary sine Gordon field theory.

Boundary sine-Gordon field theory. — We consider a semiopen chain with the Hamiltonian

$$\mathcal{H} = \sum_{j<0} \left[J\boldsymbol{S}_j \cdot \boldsymbol{S}_{j-1} - \mu_B \boldsymbol{H} \cdot \mathbf{g} \cdot \boldsymbol{S}_j + (-1)^j \boldsymbol{D} \cdot \boldsymbol{S}_j \times \boldsymbol{S}_{j-1} \right], \tag{1}$$

which models one side of an infinite chain broken by a nonmagnetic impurity at $j = 0$. $\mathbf{g}$ is the g tensor of localized spins, and μ_B is Bohr magneton.

The Zeeman energy can be represented as $-\mu_B \sum_{j,a,b} H^a \left[g^u_{ab} + (-1)^j g^s_{ab} \right] S^b_j$. Hereafter, we assume that $g^u_{ab} g \delta_{ab}$ and $|g^s_{ab}| \ll g$, and employ a unit $\hbar = k_B = g\mu_B = 1$.

We consider $\boldsymbol{H} = H\hat{z}$ applied along the z direction ($\hat{z}$ is a unit vector in the z direction). The last term of (1) is the staggered Dzyaloshinskii-Moriya (DM) interaction. This can be eliminated by a staggered rotation of spin about the direction of $\boldsymbol{D}$ by angle $(-1)^j \alpha/2$, where $\alpha = \tan^{-1}(|\boldsymbol{D}|/J)$ where j is the site index.

Under an applied field, this transformation leaves a staggered field $\boldsymbol{h} \sim \boldsymbol{H} \times \boldsymbol{D}/2$, which is perpendicular to $\boldsymbol{H}$ and to $\boldsymbol{D}$. [5, 6] Together with the staggered field due to the staggered component of the g tensor, the effective model may be given by

$$\mathcal{H} = \sum_{j<0} \left[J\boldsymbol{S}_j \cdot \boldsymbol{S}_{j-1} - HS^z_j - h(-1)^j S^x_j \right], \tag{2}$$

keeping only the most important terms. $h = c_s H$ is the effective staggered field, approximately perpendicular to the applied field; the direction of the staggered field is chosen to be the x axis. c_s depends both on the staggered DM interaction and on the staggered part of g tensor g^s_{ab}.

Using bosonization formulas,

$$S^z_x \sim m + \frac{1}{2\pi R}\partial_x\phi + C^z_s(-1)^x \cos(\phi/R + Hx), \quad (3)$$

$$S^\pm_x \sim e^{\pm 2\pi R i\tilde{\phi}}\left[C^\perp_s(-1)^x + C^\perp_u \cos(\phi/R + Hx)\right], \quad (4)$$

at low temperature $T \ll J$, the model (2) is mapped to a boundary sine Gordon (BSG) field theory, defined by the action

$$\mathcal{A} = \int_{-\infty}^{\infty} dt \int_{-\infty}^{0} dx \left[\frac{1}{2}\left\{\frac{1}{v^2}(\partial_t\tilde{\phi})^2 - (\partial_x\tilde{\phi})^2\right\} - C^\perp_s h \cos(2\pi R\tilde{\phi})\right]. \quad (5)$$

v is the spin-wave velocity. The fields ϕ and $\tilde{\phi}$ are dual and compactified as $\phi \sim \phi + 2\pi R$ and $\tilde{\phi} \sim \tilde{\phi} + 1/R$; m is the uniform magnetization density and the nonuniversal constants $C^z_{u,s}$ and $C^\perp_{u,s}$ are determined numerically [18]. The bulk operator $\cos(2\pi R\tilde{\phi})$, which represents the transverse staggered magnetization, is relevant in the renormalization group sense. Thus it induces a finite mass (excitation gap), as it was observed in the experiments. [5, 6] The bulk gap is stable against dilute nonmagnetic impurities.

In the absence of the staggered field term, the field ϕ obeys the Dirichlet boundary condition $\phi(x = 0, t) =$ const. [19]. This is equivalent to the Neumann boundary condition in terms of the dual field:

$$\partial_x\tilde{\phi}(x,t)\Big|_{x=0} = 0. \quad (6)$$

Inclusion of the staggered field could change the boundary condition; in fact, the staggered field in the bulk would also induce the corresponding operator $\cos(2\pi R\tilde{\phi})$ at the boundary. If this boundary perturbation is dominant, $\tilde{\phi}$ would obey the Dirichlet boundary condition. However, since $\cos(2\pi R\tilde{\phi})$ is, as a boundary operator, (nearly) marginal in RG, its effects are negligible at the energy scale set by the bulk spin gap. Thus, for a small staggered field h, the boundary condition can still be regarded as the Neumann on $\tilde{\phi}$.

Energy spectrum. — The elementary excitation of the bulk sine Gordon field theory includes soliton (denoted by S) and antisoliton ($\bar{S}$) with the same mass M. A soliton and antisoliton carry soliton charge $Q = +1$ and $Q = -1$, respectively. Additional particles called breathers are generated as bound states of a soliton and an antisoliton [20, 21]. There can be several different kinds of breathers B_n with the mass $M_n = 2M\sin(n\pi\xi/2)$, for $n = 1, 2, \ldots, \lfloor\xi^{-1}\rfloor$. Here $\lfloor\cdot\rfloor$ is the floor function. Breathers have zero soliton charge. The soliton charge is conserved in the bulk sine Gordon field theory. For the case of our interest, that is experimental situations in $KCuGaF_6$ and Cu-PM, the parameter $\xi = 1/(2/\pi R^2 - 1)$ satisfies $\xi < 1/3$. In particular, $\xi \approx 1/3$ in the low field limit $H \to 0$.

Fortunately, the BSG theory (5) with the Neumann boundary condition (6) is still integrable [9]. An analysis of the *boundary* S matrices implies [9–12, 22] the existence of the BBS with the mass

$$M_{\rm BBS} = M\sin(\pi\xi), \quad (7)$$

for $\xi < 1/2$. Therefore, the BBS with $M_{\rm BBS} \sim \sqrt{3}M/2$ does exist in the low field limit of the present system. The BBS of soliton, antisoliton, and first breather turn out to be identical and there is only one type of BBS. This is another manifestation of the soliton charge nonconservation at the boundary.

Thus the analysis of the BSG theory predicts a new excited state, which is a BBS, at the energy $M_{\rm BBS}$ lower than the bulk gap M. In fact, in an earlier numerical study of an open chain based on density matrix renormalization group, Lou *et al.* [23, 24] had found such an excited state localized near the boundary. They called it a midgap state. Figure 1 shows a comparison of the soliton (12) and BBS (7) masses, to the numerically obtained bulk gap and the energy of the midgap state in Refs. [23, 24]. Here we used $M \approx 1.85\,(h/J)^{2/3}[\ln(J/h)]^{1/6}$ appropriate for $H = 0$, which was used in Refs. [23, 24]. The excellent agreement between the two energies means that the midgap state found in the DMRG calculation was nothing but a BBS.

While it was pointed out in Refs. [23, 24] that the midgap state is localized near the boundary, physical understanding of its origin has been lacking. The analogy to the edge state in the Haldane phase is clearly inappropriate, since the $S = 1/2$ HAFM in a staggered field is topologically trivial. With the present identification of the midgap state with the BBS, the BSG theory is established as an effective theory describing the boundary physics of the system. This is essential in understanding the ESR spectra.

Electron spin resonance. — Next we discuss the ESR spectrum, which is given by $I(\omega) \propto \omega\chi''_{\rm phys}(q = 0, \omega)$. Here, χ'' is an imaginary part of the dynamical susceptibility χ. $\chi_{+-}(q,\omega) = -G_{S^+S^-}(q, i\omega = \omega + i\epsilon)$ where positive infinitesimal ϵ is the analytic continuation of the

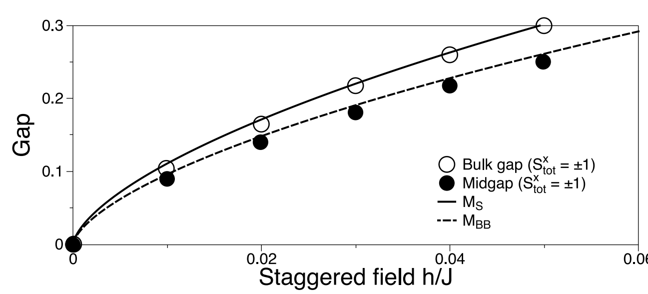

Figure 1. Numerically obtained bulk gap (open circles) and midgap (solid circles) in [23] are compared with the soliton mass M and the BBS mass $M_{\rm BBS}$ (7).

temperature Green's function $G_{S^+S^-}(q, i\omega)$. The staggered rotation of spins by angles $(-1)^j\alpha/2$ to eliminate the DM interaction mix the uniform ($q = 0$) and the staggered ($q = \pi$) components. The physical susceptibility $\chi''_{\rm phys}(q = 0, \omega)$ is

$$\chi''_{\rm phys}(0, \omega) \sim \chi''_{+-}(0, \omega) + \left(\frac{D_z}{J}\right)^2 \chi''_{+-}(\pi, \omega), \tag{8}$$

where D_z is the z component of the DM vector $\boldsymbol{D}$ parallel to the applied field. On the right-hand side, we dropped the longitudinal susceptibility $\chi_{zz}(q = \pi, \omega)$ because it contains the same resonances as those in the transverse part $\chi_{+-}(q = 0, \omega)$, and merely modifies their intensities.

Let us first review the ESR in the bulk, in the limit of $T \to 0$. The uniform part $\chi''_{+-}(0, \omega)$ reflects transitions caused by the operator

$$S^{\pm}_{q=0} \sim e^{\pm 2\pi R i\tilde{\phi}} \cos(\phi/R + Hx). \tag{9}$$

The operator $\cos(\phi/R)$ changes the soliton charge by ± 1, and thus must create at least one soliton or antisoliton. The other factor $e^{\pm 2\pi R i\tilde{\phi}}$ can create any number of excitations with zero soliton charge in total. Thus ESR induced by the operator (9) with the lowest possible energy corresponds to creation of a single soliton or antisoliton. It should be also noted that the factor Hx in the cosine causes the shift of the momentum with H. That is, the created soliton or antisoliton should carry the momentum H. Thus the ESR due to a single soliton/antisoliton creation is at frequency $\omega = E_S \equiv \sqrt{M^2 + H^2}$. There are also resonances due to (9) at higher energies, corresponding to creation of additional elementary excitations.

Next we turn to the staggered part $\chi''_{+-}(q = \pi, \omega)$, which reflects transitions caused by the operator

$$S^{\pm}_{q=\pi} \sim e^{\pm 2\pi R i\tilde{\phi}}. \tag{10}$$

This carries zero soliton charge, and thus the simplest excitation induced by this operator is creation of a single breather B_n. This leads to the resonances at $\omega = M_n$.

Now let us discuss the boundary effects on ESR. Here we discuss the ESR spectrum based on physical picture, leaving systematic formulations to the Supplementary Material .

First we consider the contribution of the staggered part $\chi''_{+-}(q = \pi, \omega)$. The simplest excitation created by the operator (10) is a single breather. In the presence of the boundary, the first breather can form the BBS. Thus the resonance with the lowest energy in the presence of the boundary is given by $\omega = M_{\rm BBS}$. Creation of a breather not bounded at the boundary and the BBS is also possible, leading to the resonance at $\omega = M_{BBS} + M_n$.

In order to understand the boundary effects on ESR, we need to clarify the issue of the momentum conservation. In general, total momentum is conserved due to the translation invariance of the system. In the presence of the boundary, the translation invariance is lost and the total momentum is no longer conserved. Nevertheless, the momentum is still important in discussing ESR spectra, because the momentum of each elementary excitation is conserved or reversed in a scattering with another elementary excitation, or in a reflection at the boundary. Thus, once created, the set of momenta of elementary excitations is conserved, up to the sign of each momentum.

	Bulk	Boundary
$T = 0$	$\omega = E_S, E_S + M_n$	$\omega = E_n, E_S + M_{\rm BBS}, E_n + M_{\rm BBS}$
$T > 0$	$\omega = \lvert E_S - M_n\rvert$	$\omega = E_n - M_{\rm BBS}$

Table I. Typical resonance modes in $\chi''_{+-}(q = 0, \omega)$. Resonances shown in the second row are absent at $T = 0$. The soliton resonance E_S is accompanied with all bulk resonances. On the other hand, E_S does not necessarily appear in the boundary resonances. In fact, some boundary resonances are involved with a novel resonance E_n instead of E_S.

	Bulk	Boundary
$T = 0$	$\omega = M_n, M_n + M_m$	$\omega = M_{\rm BBS}, M_n + M_{\rm BBS}$
$T > 0$	$\omega = M_n - M_m\ (n > m)$	$\omega = M_n - M_{\rm BBS}$

Table II. Typical resonance modes in $\chi''_{+-}(q = \pi, \omega)$. Breather masses are directly measured in the bulk part. The BBS mass itself appears in the boundary resonances. Equations (8) shows that intensities of these modes are smaller than those in Table I by $(D_z/J)^2$.

The existence of the boundary has an interesting effect, in addition to the contribution of the BBS, on the ESR spectrum. Although the expectation of the operator $\cos(\phi/R)$ vanishes in the bulk, it is nonvanishing [25, 26] near a boundary with the Dirichlet boundary condition on ϕ [equivalent to the Neumann boundary condition (6) on $\tilde{\phi}$]. This reflects ϕ taking a fixed value at the boundary. Thus, *in the vicinity of the boundary*, the leading contribution from the uniform part is effectively given by the operator $S^{\pm}_{q=0} \sim e^{\pm 2\pi R i\tilde{\phi}} \cos(Hx)$, which creates excitations with zero soliton charge, in contrast to the original one (9). This is another consequence of violation of soliton charge conservation at the boundary. The created excitations should carry the total momentum $\pm H$, up to the uncertainty $\sim 1/l_p$. Here l_p is the pinning lengths cale, namely $\phi(x) \sim$ const. if $|x| < l_p$.

Thus, the simplest among the possible ESR processes due to this operator is the creation of a single breather B_n with momentum $\pm H$. This corresponds to the frequency

$$E_n = \sqrt{{M_n}^2 + H^2}. \tag{11}$$

The resonance at E_n with $n > 1$ was absent in the bulk and is a new feature due to the boundary. We emphasize that, these new resonances do *not* simply follow from

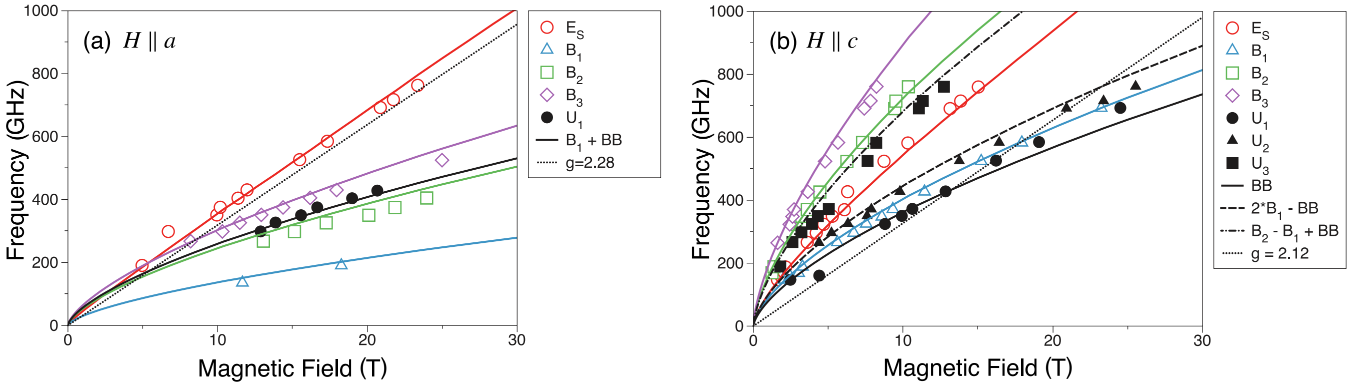

Figure 2. (color online) Frequency vs field diagrams of ESR in $\mathrm{KCuGaF_6}$ [15] for (a) $H \parallel a$ and (b) $H \parallel c$ configurations. The dotted line is high temperature paramagnetic resonance $\omega = H$. Open symbols and filled symbols represent bulk modes and "unknown modes." $\mathrm{E_S, B_1, B_2, B_3}$ denotes resonances $\omega = E_S, M_1, M_2, M_3$ by a soliton S and breathers B_n. An antisoliton $\bar{S}$ also leads to $\omega = E_S$. The labels U_1, U_2, U_3 are "unknown" peaks found in [15]. (a) The configuration $H \parallel a$ bears the smallest $h = c_s H$ with the coefficient $c_s = 0.031$. An excitation $\omega = M_1 + M_{\mathrm{BBS}}$ is found in addition to the bulk excitations. (b) We have the largest staggered field, $c_s = 0.178$, when $H \parallel c$. This large c_s makes the rich kinds of boundary modes detectable. The labels BB, 2*B$_1$-BB, B$_2$-B$_1$+BB denote $\omega = M_{\mathrm{BBS}}, 2M_1 - M_{\mathrm{BBS}}, M_2 - M_1 + M_{\mathrm{BBS}}$.

the existence of the midgap state numerically found in Refs. [23, 24]. In fact, the resonance frequency E_n does not explicitly contain the energy M_{BBS}. This shows the necessity of the BSG framework to fully understand the physics at the boundary.

At finite temperatures, additional resonances may be observable. When the initial state contains the BBS as a thermal excitation, a resonance at $\omega = M_n - M_{\mathrm{BBS}}$ exists, corresponding to annihilation of the BBS and creation of a breather B_n. Similarly, when the initial state contains B_1, the resonance at $\omega = M_n - M_1 + M_{\mathrm{BBS}}$ corresponds to the creation of B_n and binding of B_1 at the boundary. These resonances are contained in the staggered part $\chi''_{+-}(\pi, \omega)$. The uniform part also contains, at finite temperatures, additional resonances.

Typical resonance modes are summarized in Tables I and II. Note that intensities of resonances due to the staggered part $\chi''_{+-}(q = \pi, \omega)$ and $\chi''_{zz}(q = \pi, \omega)$ are suppressed by the factor $(D_z/J)^2$ in (8), compared to those from the uniform part $\chi''_{+-}(q = 0, \pi)$.

Comparison with experiments. — Thus several novel resonances, which are absent in the bulk, are derived from the BSG theory. They indeed match the "unknown" resonances observed previously in ESR spectra on $\mathrm{KCuGaF_6}$ (Figure 2) and Cu-PM (Figure 3). Here the uniform field effect is taken into account in the soliton-antisoliton mass [27],

$$M = \frac{2v}{\sqrt{\pi}} \frac{\Gamma(\xi/2)}{\Gamma((1+\xi)/2)} \left[\frac{\Gamma(1/(1+\xi))}{\Gamma(\xi/(1+\xi))} \frac{C_s^{\perp}\pi}{2v} c_s H \right]^{(1+\xi)/2}. \tag{12}$$

While the ratio $c_s = h/H$ can in principle be determined by the staggered DM interaction and g tensor, we use the value obtained by fitting experimental data.

Each figure shows different resonances, though. The difference between the spectra in two materials can be understood in terms of the different magnitude of the DM interaction. The coefficient c_s at its maximum is larger (0.178) in $\mathrm{KCuGaF_6}$ compared to 0.083 in Cu-PM. While precise estimates of the DM interaction and the staggered g tensor are not available, the staggered DM interaction is presumably larger in $\mathrm{KCuGaF_6}$. This leads to larger mixing of the staggered part $\chi''_{+-}(q = \pi, \omega)$. Thus it is natural that the resonances due to the mixings are observed only in $\mathrm{KCuGaF_6}$ (Fig. 2). We note that, the simplest possible BBS contribution at $\omega = M_{\mathrm{BBS}}$ is not observed for $H \parallel a$ in Fig. 2 (a). This is presumably because only two of the frequencies used in the experiments can detect the resonance below the bulk resonance at $\omega = M_1$. On the other hand, in the Cu-PM with a smaller DM interaction, only the contributions from the

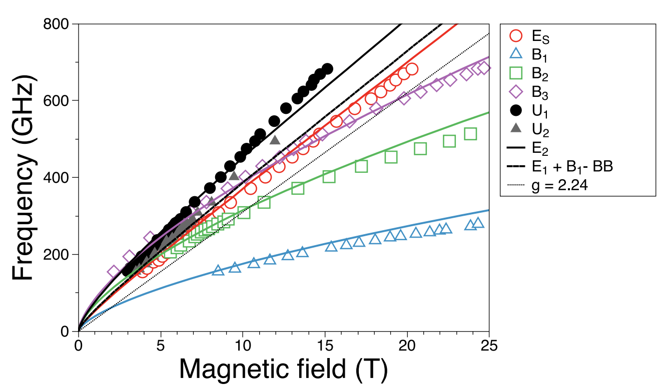

Figure 3. (color online) Frequency vs field diagrams of ESR in Cu-PM [16]. Two "unknown" peaks U_1 and U_2 are attributed to $\omega = E_2$, $E_1 + M_1 - M_{\mathrm{BBS}}$ respectively, where E_n is defined in Eq.(11). These boundary modes appear in $\chi''_{xx}(q = 0, \omega)$.

uniform part are observed (Fig. 3). We conjecture that, with more careful examination of the spectra, more resonances due to the BBS will be found in experiments.

Conclusions. — We point out the existence of BBS and modification of the selection rules at boundaries of the $S = 1/2$ antiferromagnetic chain in an effective staggered field, in terms of the BSG theory (5). The boundary effects can account for the mysterious "unknown modes" found in two compounds $KCuGaF_6$ [15] and Cu-PM [16, 17].

In the compound $KCuGaF_6$, magnetic ions Cu^{2+} and nonmagnetic ions Ga^{3+} form a pyrochlore lattice. Magnetically, the compound $KCuGaF_6$ is effectively regarded as $S = 1/2$ HAFM chains of Cu^{2+} ions. However, since Cu^{2+} and Ga^{3+} ions occupy equivalent positions, an intersite mixing of them can occur in the course of syntheses [28]. We speculate that the intersite mixing brings about nonmagnetic impurities in spin chains. We expect that a few percent of the nonmagnetic impurities would lead to observation of the boundary resonances as discussed in this Letter. Our picture may be verified experimentally by controlling the density of nonmagnetic impurity, which will change the intensity of boundary resonances.

The authors thank P. Bouillot, T. Giamarchi, S. Takayoshi, H. Tanaka, I. Umegaki, and S. Zvyagin for fruitful discussions. This work is partly supported by the Global COE Program "The Physical Sciences Frontier" (S.C.F.), and KAKENHI Grant No. 50262043 from MEXT of Japan.

[1] M. Hagiwara, K. Katsumata, I. Affleck, B. I. Halperin, and J. P. Renard, Phys. Rev. Lett. **65**, 3181 (1990).
[2] C. D. Batista, K. Hallberg, and A. A. Aligia, Phys. Rev. B **60**, R12553 (1999).
[3] M. Yoshida, K. Shiraki, S. Okubo, H. Ohta, T. Ito, H. Takagi, M. Kaburagi, and Y. Ajiro, Phys. Rev. Lett. **95**, 117202 (2005).
[4] D. C. Dender, P. R. Hammar, D. H. Reich, C. Broholm, and G. Aeppli, Phys. Rev. Lett. **79**, 1750 (1997).
[5] M. Oshikawa and I. Affleck, Phys. Rev. Lett. **79**, 2883 (1997).
[6] I. Affleck and M. Oshikawa, Phys. Rev. B **60**, 1038 (1999).
[7] A. B. Zamolodchikov, Int. J. Mod. Phys. A **4**, 4235 (1989).
[8] R. Coldea, D. A. Tennant, E. M. Wheeler, E. Wawrzynska, D. Prabhakaran, M. Telling, K. Habicht, P. Smeibidl, and K. Kiefer, Science **327**, 177 (2010).
[9] S. Ghoshal and A. Zamolodchikov, Int. J. Mod. Phys. A **9**, 3841 (1994).
[10] S. Ghoshal, Int. J. Mod. Phys. A **9**, 4801 (1994).
[11] P. Mattsson and P. Dorey, J. Phys. A **33**, 9065 (2000).
[12] Z. Bajnok, L. Palla, and G. Takács, Nucl. Phys. **B614**, 405 (2001).
[13] D. Schuricht, F. H. L. Essler, A. Jaefari, and E. Fradkin, Phys. Rev. Lett. **101**, 086403 (2008).
[14] D. Schuricht, F. H. L. Essler, A. Jaefari, and E. Fradkin, Phys. Rev. B **83**, 035111 (2011).
[15] I. Umegaki, H. Tanaka, T. Ono, H. Uekusa, and H. Nojiri, Phys. Rev. B **79**, 184401 (2009).
[16] S. A. Zvyagin, A. K. Kolezhuk, J. Krzystek, and R. Feyerherm, Phys. Rev. Lett. **93**, 027201 (2004).
[17] S. A. Zvyagin, E. Čižmár, M. Ozerov, J. Wosnitza, R. Feyerherm, S. R. Manmana, and F. Mila, Phys. Rev. B **83**, 060409 (2011).
[18] T. Hikihara and A. Furusaki, Phys. Rev. B **69**, 064427 (2004).
[19] S. Eggert and I. Affleck, Phys. Rev. B **46**, 10866 (1992).
[20] R. F. Dashen, B. Hasslacher, and A. Neveu, Phys. Rev. D **11**, 3424 (1975).
[21] A. B. Zamolodchikov and A. B. Zamolodchikov, Ann. Phys. **120**, 253 (1979).
[22] D. Schuricht and F. H. L. Essler, J. Stat. Mech. **2007**, P11004 (2007).
[23] J. Lou, C. Chen, J. Zhao, X. Wang, T. Xiang, Z. Su, and L. Yu, Phys. Rev. Lett. **94**, 217207 (2005).
[24] J. Lou, C. Chen, and X. Wang, Phys. Rev. B **73**, 092407 (2006).
[25] S. Fujimoto and S. Eggert, Phys. Rev. Lett. **92**, 037206 (2004).
[26] S. Fujimoto and S. Eggert, Phys. Rev. Lett. **100**, 059904(E) (2008).
[27] S. Lukyanov and A. Zamolodchikov, Nucl. Phys. **B493**, 571 (1997).
[28] I. Umegaki and H. Tanaka, (private communications).

Supplemental Material to
"Boundary Resonances in $S = 1/2$ Antiferromagnetic Chains under a Staggered Field"

EFFECTIVE LATTICE MODEL

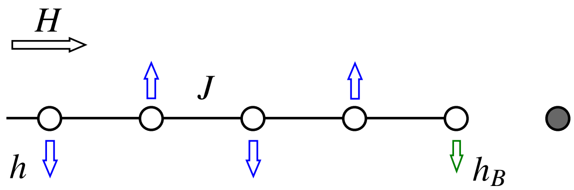

Figure 4. Semi-infinite Heisenberg antiferromagnetic chain with an effective staggered field, cut by a non-magnetic impurity (the gray filled circle).

We derive the effective lattice model (2) of the main text, with an emphasis on the mixing of $q = \pi$ modes through the transformation eliminating the DM interaction. First we consider the model Hamiltonian

$$\mathcal{H}_0 = \sum_{j \le 0} \left[J \boldsymbol{S}_j \cdot \boldsymbol{S}_{j-1} - H S_j^z + (-1)^j \boldsymbol{D} \cdot \boldsymbol{S}_j \times \boldsymbol{S}_{j-1} \right]. \quad (13)$$

Here, for simplicity, the effects of the anisotropic g tensor are ignored, and they will be taken into account later. We rotate the spin $\boldsymbol{S}_j$ about the direction of $\boldsymbol{D}$ by the angle $(-1)^j \alpha/2$ where $\alpha = \tan^{-1}(|\boldsymbol{D}|/J)$. When $|\boldsymbol{D}| \ll J$, $\alpha \ll 1$ and the transformation of the spin operator can be linearized as

$$\boldsymbol{S}_j \to \boldsymbol{S}_j + (-1)^j \frac{\boldsymbol{D}}{2J} \times \boldsymbol{S}_j. \quad (14)$$

Thus, in the presence of the uniform applied field $\boldsymbol{H}$, a staggered field perpendicular to both $\boldsymbol{H}$ and $\boldsymbol{D}$ is generated.

In addition, the staggered component of g tensor also contributes to generating the staggered field. In contrast to the one due to the staggered DM interaction, the staggered field coming from the staggered component of the g tensor is not necessarily perpendicular to the applied field. However, in the effective field theory description, the longitudinal component of the staggered field accompanies an oscillating factor, which makes it vanish upon spatial integration. Thus it can be ignored for the purpose of discussion of gap opening, and only the transverse staggered field has to be considered.

Therefore, the $S = 1/2$ antiferromagnetic chain under an applied magnetic field, with both staggered g tensor and staggered DM interaction can be described by the effective lattice model (2) of the main text. The effective staggered field h depends on both the staggered DM interaction and the staggered g tensor.

In the course of eliminating the staggered DM interaction, the spin operator is transformed according to Eq. (14). This has to be taken into account in the discussion of physical susceptibility. Namely, the physical uniform susceptibility $\chi''_{\mathrm{phys}}(q = 0, \omega)$ has contributions from both uniform and staggered susceptibilities calculated for the effective model after the elimination of the DM interaction:

$$\chi''_{\mathrm{phys}}(q = 0, \omega) \sim \chi''_{+-}(q = 0, \omega) + \left(\frac{D_z}{J}\right)^2 \chi''_{+-}(q = \pi, \omega) + \left(\frac{D_\perp}{J}\right)^2 \chi''_{zz}(q = \pi, \omega), \quad (15)$$

where $D_\perp$ is the magnitude of the component $\boldsymbol{D}$ perpendicular to the z axis. As we will see below, the longitudinal susceptibility $\chi''_{zz}(q = \pi, \omega)$ adds no resonant peak to the former two susceptibilities. The longitudinal staggered susceptibility just modifies intensities of the transverse susceptibilities.

Fig. 4 shows a schematic picture of the staggered fields generated from the external uniform field H, in the bulk (h) and at the boundary (h_B). Note that the boundary staggered field h_B, coupled to the end spin S_0^x, is indistinguishable to the bulk staggered field h in the lattice model. But their behaviors under renormalization group (RG) transformations are quite different.

RG ANALYSIS

The bosonization of spins leads to an effective boundary field theory with an action,

$$\mathcal{A} = \int_{-\infty}^{\infty} dt \int_{-\infty}^{0} dx \left[\frac{1}{2} \left\{ \frac{1}{v^2} (\partial_t \tilde{\phi})^2 - (\partial_x \tilde{\phi})^2 \right\} - C_s^\perp h \cos(2\pi R \tilde{\phi}) \right] - C_s^\perp h_B \int_{-\infty}^{\infty} dt \, \cos\left[2\pi R \tilde{\phi}(x = 0)\right]. \quad (16)$$

Scaling dimensions of the bulk and boundary staggered magnetizations are respectively

$$x_h = \pi R^2, \qquad x_{h_B} = 2\pi R^2. \quad (17)$$

When the uniform field H is zero, the effective lattice model (2) in the paper is SU(2) symmetric, where the compactification radius R is given by $R = 1/\sqrt{2\pi}$. As the uniform and staggered fields increase, the compactification radius decreases [1]. Recall that a bulk operator is relevant (irrelevant) when its scaling dimension is smaller (bigger) than 2, and a boundary operator is relevant (irrelevant) when its scaling dimension is smaller (bigger) than 1. Thus, both the bulk ($x_h \le 1/2$) and

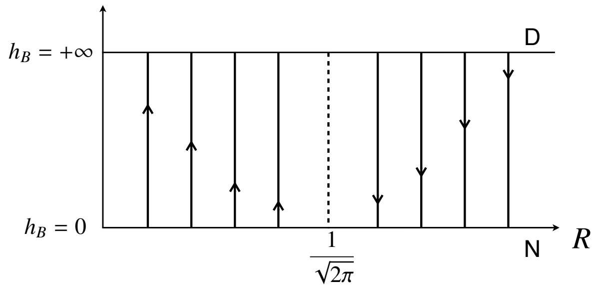

Figure 5. The boundary RG flow. On the line $h_B = 0$ denoted by "N", the boundary condition is Neumann. On the line $h_B = +\infty$ denoted by "D", the boundary condition is Dirichlet.

boundary ($x_{h_B} \leq 1$) staggered magnetizations are relevant. The boundary staggered magnetization is marginal at zero field $H = 0$. The boundary RG flow is shown in Fig. 5. The line $h_B = 0$ corresponds to the Neumann boundary condition. In the presence of the boundary staggered field, the boundary condition is neither Neumann nor Dirichlet:

$$\partial_x \tilde{\phi}(x,t)\Big|_{x=0} = 2\pi R C_s^{\perp} h_B \sin\big[2\pi R \tilde{\phi}(x=0,t)\big] \tag{18}$$

$h_B = +\infty$ corresponds to the Dirichlet boundary condition because the field $\tilde{\phi}(x=0,t)$ is pinned to a certain value in order to optimize the potential energy $\propto h_B \cos[2\pi R\tilde{\phi}(x=0,t)]$.

As we perform the RG transformation iteratively, the bulk staggered field h grows rapidly. When the effective coupling h/J becomes $\mathcal{O}(1)$, the RG transformation breaks down. On the other hand, the boundary staggered field h_B/J is still much smaller than 1 after the iterative RG transformations because the boundary staggered magnetization is almost marginal. Therefore, at the lowest order approximation, we may ignore the boundary staggered field h. Finally we reach the effective action of the boundary sine Gordon model (5) together with the boundary condition (6), in the main text.

BOUNDARY BOUND STATE

Here, following Refs. [2, 3], we briefly review the energy spectrum of the boundary sine Gordon model with the Neumann condition. The energy spectrum in bulk is the same as those in the conventional sine Gordon model. A soliton (denoted as S) and an antisoliton (denoted as $\bar{S}$) exist and several breathers are formed as bound states of one soliton and one antisoliton. One can know that masses of breathers by analyzing simple poles of the exact S matrix. As is well known, the S matrix characterizes

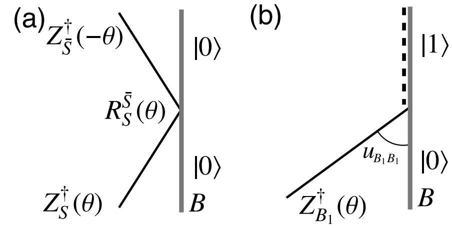

Figure 6. (a) A reflection process at the boundary. The boundary is represented as an infinitely heavy particle B (thick gray line). (b) A formation of BBS using a breather B_1. The system is excited from the ground state $|0\rangle = B|\mathrm{vac}\rangle$ to the one-BBS state $|1\rangle$.

two-particle scatterings:

$$\begin{aligned}
Z_{a_1}(\theta_1) Z_{a_2}(\theta_2) &= S^{b_1 b_2}_{a_1 a_2}(\theta_1 - \theta_2) Z_{b_2}(\theta_2) Z_{b_1}(\theta_1) \\
Z^\dagger_{a_1}(\theta_1) Z^\dagger_{a_2}(\theta_2) &= S^{b_1 b_2}_{a_1 a_2}(\theta_1 - \theta_2) Z^\dagger_{b_2}(\theta_2) Z^\dagger_{b_1}(\theta_1) \\
Z_{a_1}(\theta_1) Z^\dagger_{a_2}(\theta_2) &= 2\pi \delta_{a_1 a_2} \delta(\theta_1 - \theta_2) \\
&\quad + S^{b_2 a_1}_{a_2 b_1}(\theta_1 - \theta_2) Z^\dagger_{b_2}(\theta_2) Z_{b_1}(\theta_1)
\end{aligned}$$

Operators $Z_a(\theta)$ and $Z^\dagger_a(\theta)$ are called as Faddeev-Zamolodchikov (FZ) operators. The parameter θ is called as a rapidity, which parameterize the energy E_a and the momentum P_a of a particle with an index a as

$$E_a(\theta) = M_a \cosh\theta, \quad P_a(\theta) = M_a \sinh\theta.$$

Since every scattering in integrable field theories is factorizable to several two-particle scatterings, the S matrix determines whole energy spectrum in bulk. An n-th breather has a mass,

$$M_n = 2M \sin\left(\frac{n\pi\xi}{2}\right), \tag{19}$$

for $n = 1, 2, \cdots, \lfloor \xi^{-1} \rfloor$. Since breathers are formed by a soliton and an antisoliton with the degenerate mass M, the mass of the breather M_n is smaller than $2M$.

Similar procedure is applicable to investigate the energy spectrum at the boundary. The scattering at the boundary is shown in Fig. 6 (a). The spatial boundary is regarded as an infinitely heavy particle B.

$$Z^\dagger_a(\theta) B = R^b_{\bar{a}}(\theta) Z^\dagger_b(-\theta) B \tag{20}$$

The index $\bar{a}$ represents the anti-particle of the particle a. The reflection factor $R^b_{\bar{a}}(\theta)$ has been studied in detail [3]. Simple poles of the reflection factor $R^b_{\bar{a}}(\theta)$ represents energy levels localized at the boundary, called as a boundary bound state (BBS).

For later convenience, we consider a rotated reflection factor

$$K^{ab}(\theta) \equiv R^b_{\bar{a}}\left(\frac{i\pi}{2} - \theta\right). \tag{21}$$

According to Ref. [3], the rotated reflection factor $K^{ab}(\theta)$ has the following simple poles $\theta = iu_{ab}$ within the physical strip $0 < \mathrm{Im}\,\theta < \pi/2$,

$$u_{ab} = u_{SS} \equiv \pi\xi, \qquad (a, b = S, \bar{S}) \tag{22}$$

$$u_{ab} = u_{B_1B_1} \equiv \frac{\pi}{2} - \frac{\pi\xi}{2}, \qquad (a = b = B_1). \tag{23}$$

Here we assumed the experimentally realized situation $3 < \xi^{-1} < 4$. Both poles (22) and (23) lead to the same BBS. In fact, the excitation gap of the BBS, M_{BBS}, is derived by the following two manners.

1. One soliton S or one antisoliton $\bar{S}$ forms a BBS:

$$M_{\mathrm{BBS}} = M \sin u_{SS} = M \sin(\pi\xi). \tag{24}$$

2. One first breather B_1 forms a BBS:

$$M_{\mathrm{BBS}} = M_1 \sin u_{B_1B_1} = M \sin(\pi\xi). \tag{25}$$

In (25), we used the relation (19). The formation of a BBS is sketched in Fig. 6 (b). Note that the BBS is formed by a soliton with the mass M or by a first breather with the mass M_1. The mass of the BBS should be smaller than $\min\{M, M_1\}$. Since $\min\{M, M_1\}$ is the lowest excitation gap, the BBS appears below the bulk gap.

CORRELATION FUNCTIONS

We summarize correlation functions in the presence of the boundary. In the Euclidean space, a two-point correlation function $G_{S^+S^-}(x_1, x_2, \tau)$ depends on two spatial variables x_1 and x_2 because the translational symmetry is broken by the boundary (impurity). For a systematic treatment, it is useful to make a Wick rotation to regard the spatial variable x as the "time", and τ as the "space" variable. In this framework,

$$G_{S^+S^-}(x_1, x_2, \tau) = \frac{\langle \mathrm{vac}|T_x S^+(x_1, \tau) S^-(x_2, 0)|\mathcal{B}\rangle}{\langle \mathrm{vac}|\mathcal{B}\rangle} \tag{26}$$

The state $|\mathrm{vac}\rangle$ is the ground state (with length given by the inverse temperature of the original system, and with the periodic boundary conditions). The symbol T_x denots the x ordering, that is, the ordering which orders operators with larger x_i to right. Note that the spin $S^a(x, \tau)$ is related to $S^a(0, 0)$ via

$$S^a(x, \tau) = e^{-xE} e^{-i\tau P} S^a(0, 0) e^{i\tau P} e^{xP},$$

where E and P are the total energy and the total momentum respectively. The state $|\mathcal{B}\rangle$ is called as a boundary state written in FZ operators and the rotated reflection factor [2].

$$\begin{aligned}|\mathcal{B}\rangle &= e^{K}|\mathrm{vac}\rangle \\ &= \exp\left[\frac{1}{2}\sum_{a,b}\int_{-\infty}^{\infty}\frac{d\theta}{2\pi}K^{ab}(\theta) Z_a^\dagger(-\theta) Z_b^\dagger(\theta)\right]|\mathrm{vac}\rangle.\end{aligned} \tag{27}$$

The Fourier transform of the x-ordered correlation function is given by

$$\begin{aligned}&G_{S^+S^-}(q, i\bar{\omega}) \\ &= \frac{1}{N}\int_0^{\infty} d\tau \int_{-\infty}^{0} dr dX\, e^{i(\bar{\omega}\tau - qr)} G_{S^+S^-}(x_1, x_2, \tau).\end{aligned} \tag{28}$$

where $\bar{\omega}$ is the Matsubara frequency. Instead of spatial variables x_1 and x_2, we used $r = -|x_1 - x_2|$ and $X = (x_1 + x_2)/2$. The infinitely large N represents the length of the semi-infinite spin chain and the coefficient $1/N$ can be understood as a density of non-magnetic impurities. When we compute dynamical susceptibility, we perform the analytic continuation $i\bar{\omega} \to \omega + i\epsilon$, where ϵ is positive infinitesimal.

BULK RESONANCES

Here we derive several resonant peaks in the ESR spectrum. An n-particle state $|\theta_1, \theta_2, \cdots, \theta_n\rangle_{a_1 a_2 \cdots a_n}$ and its conjugate ${}^{a_n \cdots a_2 a_1}\langle \theta_n, \cdots, \theta_2, \theta_1|$ are defined by

$$|\theta_1, \theta_2, \cdots, \theta_n\rangle_{a_1 a_2 \cdots a_n} = Z_{a_1}^\dagger(\theta_1) Z_{a_2}^\dagger(\theta_2) \cdots Z_{a_n}^\dagger(\theta_n)|\mathrm{vac}\rangle,$$
$${}^{a_n \cdots a_2 a_1}\langle \theta_n, \cdots, \theta_2, \theta_1| = \langle \mathrm{vac}|Z_{a_n}(\theta_n) \cdots Z_{a_2}(\theta_2) Z_{a_1}(\theta_1).$$

FZ operators $Z_a^\dagger(\theta)$ and $Z_a(\theta)$ respectively creates and annihilates a particle with a rapidity θ with an index $a = S, \bar{S}, B_m$. The energy $E = M_a \cosh\theta$ and the momentum $p = M_a \sinh\theta$ are parameterized by the single parameter θ. We put $v = 1$ for simplicity. The above multi-particle states are orthonormal.

$$\begin{aligned}&{}^{a_n \cdots a_1}\langle \theta_n, \cdots, \theta_1|\theta'_1, \cdots, \theta'_m\rangle_{a'_1 \cdots a'_m} \\ &= \delta_{nm}\delta_{a_1 a'_1} \cdots \delta_{a_n a'_n}(2\pi)^n \delta(\theta_1 - \theta'_1) \cdots \delta(\theta_n - \theta'_n)\end{aligned} \tag{29}$$

A set of n-particle states is complete:

$$1 = |\mathrm{vac}\rangle\langle \mathrm{vac}| + \sum_{n=1}^{\infty}\frac{1}{n!}\sum_{a_1, \cdots, a_n}\int \frac{d\theta_1 \cdots d\theta_n}{(2\pi)^n}|\theta_1, \cdots, \theta_n\rangle_{a_1 \cdots a_n}{}^{a_n \cdots a_1}\langle \theta_n, \cdots, \theta_1|. \tag{30}$$

This identity operator allows one to expand correlation functions by intermediate states. We can expand the boundary state in the power of K as

$$|\mathcal{B}\rangle = e^K|\mathrm{vac}\rangle = |\mathrm{vac}\rangle + K|\mathrm{vac}\rangle + \cdots . \tag{31}$$

Let us consider the bulk part of the correlation $G_{S^+S^-}(q=\pi, i\omega)$, that is,

$$\begin{aligned} G^{(0)}_{S^+S^-}(q=\pi, i\bar{\omega}) &= \frac{1}{N}{C_s^\perp}^2\int_0^\infty d\tau\int_{-\infty}^0 dr\int_{-\infty}^0 dX\, e^{i\bar{\omega}\tau}\langle\mathrm{vac}|T_x e^{-i2\pi R\tilde{\phi}(x_1,\tau)}e^{i2\pi R\tilde{\phi}(x_2,0)}|\mathrm{vac}\rangle \\ &= \sum_{m=1}^{\lfloor\xi^{-1}\rfloor}\frac{v{C_s^\perp}^2}{M_m}|F_{B_m}^{e^{i2\pi R\tilde{\phi}}}|^2\left(\frac{1}{i\bar{\omega}-M_m}+\frac{1}{i\bar{\omega}+M_m}\right)+\cdots . \end{aligned} \tag{32}$$

Thanks to the Lorentz invariance of the sine Gordon model, the matrix element $\langle\mathrm{vac}|e^{-i2\pi R\tilde{\phi}(x_1,\tau)}|\theta\rangle_a$ involving the intermediate state $|\theta\rangle_a$ can be computed easily.

$$\langle\mathrm{vac}|e^{-i2\pi R\tilde{\phi}(x_1,\tau)}|\theta\rangle_{B_m} = F_{B_m}^{e^{-i2\pi R\tilde{\phi}}}e^{i\tau M_m\sinh\theta + x_1 M_m\cosh\theta}$$

The factor $F_{B_m}^{e^{-i2\pi R\tilde{\phi}}} \equiv \langle\mathrm{vac}|e^{-i2\pi R\tilde{\phi}(0,0)}|\theta\rangle_{B_n}$ is a form factor of the operator $e^{-i2\pi R\tilde{\phi}}$. Form factors generally depend on the rapidity θ, but the $F_{B_m}^{e^{-i2\pi R\tilde{\phi}}}$ does not. In integrable field theories, form factors can be exactly derived. One can find several exact form factors of the sine Gordon model in Ref. 4.

After taking analytic continuation $i\bar{\omega}\to\omega+i\epsilon$, we obtain

$$\begin{aligned} &-\mathrm{Im}\,G^{(0)}_{S^+S^-}(q=\pi,\omega+i\epsilon) \\ &\quad= \sum_{n=1}^{\lfloor\xi^{-1}\rfloor}\frac{2\pi v{C_s^\perp}^2}{M_n}|F_{B_n}^{e^{i2\pi R\tilde{\phi}}}|^2\delta(\omega-M_n)+\cdots . \end{aligned} \tag{33}$$

Multi-particle resonant peaks such as $\delta(\omega-M_n-M_m)$ exist in the ignored terms. (33) leads to peaks in (15) as

$$\left(\frac{D_z}{J}\right)^2\sum_{n=1}^{\lfloor\xi^{-1}\rfloor}\frac{2\pi v{C_s^\perp}^2}{M_n}|F_{B_n}^{e^{i2\pi R\tilde{\phi}}}|^2\delta(\omega-M_n)+\cdots . \tag{34}$$

As stated in the paper, the intensity of the staggered susceptibility $\chi''_{+-}(q=\pi,\omega)$ is suppressed by the factor $(D_z/J)^2$. Bulk parts of the resonant peaks which comes from $\chi''_{+-}(0,\omega)$ and $\chi_{zz}(\pi,\omega)$ are similarly obtained, which are respectively

$$\frac{\pi v{C_u^\perp}^2}{M}|F_S^{e^{i\phi/R+i2\pi R\tilde{\phi}}}(\theta_0)|^2\delta(\omega-E_S), \tag{35}$$

$$\left(\frac{D_\perp}{J}\right)^2\frac{\pi v{C_s^z}^2}{M}|F_S^{e^{i\phi/R+i2\pi R\tilde{\phi}}}(\theta_0)|^2\delta(\omega-E_S). \tag{36}$$

$\theta_0\equiv\ln\left[\left\{H+\sqrt{M^2+H^2}\right\}/M\right]$. Both of them detect the soliton resonance at $\omega=E_S=\sqrt{M^2+H^2}$. The latter (36) has a weaker intensity by the factor $(D_\perp/J)^2$ than the former (35). The $q=\pi$ component of S_x^z,

$$S_x^z\sim C_s^z(-1)^x\cos(\phi/R+Hx),$$

is similar to the $q=0$ component of $S_x^\pm$,

$$S_x^\pm\sim C_u^\perp e^{\mp i2\pi R\tilde{\phi}}\cos(\phi/R+Hx).$$

Thus, all resonant peaks in $\chi''_{zz}(q=\pi,\omega)$ appear also in $\chi''_{+-}(q=0,\omega)$, and the latter has stronger intensities in (15). We may forget $\chi''_{zz}(q=\pi,\omega)$ when we focus on resonance frequencies

We should emphasize that the breather resonances $\delta(\omega-M_n)$ can result only from the transverse staggered component $\chi''_{+-}(q=\pi,\omega)$ in $\chi''_{\mathrm{phys}}(q=0,\omega)$. This is an important consequence of the mixing (15) caused by the staggered DM interaction. Without the mixing, we cannot observe any breather resonance.

BOUNDARY RESONANCES

Transverse staggered component $G_{S^+S^-}(q=\pi,i\omega)$

Boundary scatterings induce rich amounts of additional resonances. For instance, we consider the first order contribution in the expansion (31) to the $G_{S^+S^-}(q=\pi,i\omega)$,

$$
\begin{aligned}
&G^{(1)}_{S^+S^-}(q=\pi,i\omega)\\
&\quad=\frac{1}{N}{C_s^{\perp}}^2\int_0^\infty d\tau\int_{-\infty}^0 drdX\, e^{i\omega\tau}\frac{1}{2}\sum_{a,b}\int_{-\infty}^\infty\frac{d\theta}{2\pi}K^{ab}(\theta)\langle\mathrm{vac}|T_x e^{-i2\pi R\tilde{\phi}(x_1,\tau)}e^{i2\pi R\tilde{\phi}(x_2,0)}|-\theta,\theta\rangle_{ab} \qquad (37)\\
&\quad=\frac{1}{N}{C_s^{\perp}}^2\int_0^\infty d\tau\int_{-\infty}^0 drdX\, e^{i\omega\tau}\frac{1}{2}\sum_{a,b}\int_{-\infty}^\infty\frac{d\theta}{2\pi}K^{ab}(\theta)\sum_{n=1}^{\lfloor\xi^{-1}\rfloor}\int_{-\infty}^\infty\frac{d\theta_1}{2\pi}\\
&\qquad\times\big[\theta_H(x_2-x_1)\langle\mathrm{vac}|e^{-i2\pi R\tilde{\phi}(x_1,\tau)}|\theta_1\rangle_{B_1}{}^{B_1}\langle\theta_1|e^{i2\pi R\tilde{\phi}(x_2,0)}|-\theta,\theta\rangle_{ab}\\
&\qquad\quad+\theta_H(x_1-x_2)\langle\mathrm{vac}|e^{i2\pi R\tilde{\phi}(x_2,0)}|\theta_1\rangle_{B_1}{}^{B_1}\langle\theta_1|e^{-i2\pi R\tilde{\phi}(x_1,\tau)}|-\theta,\theta\rangle_{ab}\big]+\cdots \qquad (38)
\end{aligned}
$$

$\theta_H(x)$ is the Heaviside step function. As we reviewed above, the factor $K^{ab}(\theta)$ has simple poles in the physical strip $0\le \mathrm{Im}\,\theta<\pi/2$,

$$\operatorname*{Res}_{\theta=iu_{SS}} K^{ab}(\theta)=-if_S,\quad (a,b=S,\bar{S}), \qquad (39)$$

$$\operatorname*{Res}_{\theta=iu_{B_1B_1}} K^{ab}(\theta)=-if_{B_1},\quad (a=b=B_1), \qquad (40)$$

where u_{SS} and $u_{B_1B_1}$ are (22) and (23). The residues $-if_S$ and $-if_{B_1}$ are not derived at the moment of publication. Here we assume $f_S,f_{B_1}>0$. In the expansion of (37), the most dominant intermediate state is one-breather state $|\theta_1\rangle_{B_n}$. The singularity of $K^{ab}(\theta)$ affects (37) when and only when $n=1$ and $a=b=B_1$.

$$
\begin{aligned}
G^{(1)}_{S^+S^-}(q=\pi,i\omega)&\sim\frac{1}{N}{C_s^{\perp}}^2\int_0^\infty d\tau\int_{-\infty}^0 drdX\, e^{i\omega\tau}f_{B_1}|F^{e^{i2\pi R\tilde{\phi}}}_{B_1}|^2\\
&\quad\times\left(e^{-\tau M_1\sin u_{B_1B_1}}e^{2XM_1\cos u_{B_1B_1}}+e^{\tau M_1\sin u_{B_1B_1}}e^{2XM_1\cos u_{B_1B_1}}\right)+\cdots\\
&=\frac{v{C_s^{\perp}}^2 f_{B_1}|F^{e^{i2\pi R\tilde{\phi}}}_{B_1}|^2}{2M_1\cos u_{B_1B_1}}\left(\frac{1}{i\omega-M_1\sin u_{B_1B_1}}+\frac{1}{i\omega+M_1\sin u_{B_1B_1}}\right)+\cdots
\end{aligned}
$$

The pole $M_1\sin u_{B_1B_1}=M\sin(\pi\xi)=M_{\mathrm{BBS}}$ gives a resonance of the boundary bound state (BBS) in $\chi''_{\mathrm{phys}}(q=0,\omega)$:

$$\left(\frac{D_\perp}{J}\right)^2\frac{\pi v{C_s^{\perp}}^2 f_{B_1}|F^{e^{i2\pi R\tilde{\phi}}}_{B_1}|^2}{M_1\sin(\pi\xi/2)}\delta(\omega-M_{\mathrm{BBS}}) \qquad (41)$$

The intensity of the peak (41) has two features. (i) The intensity is suppressed by the factor $(D_\perp/J)^2$. (ii) The intensity is independent of a concentration $(1/N)$ of non-magnetic impurities. The first feature is common with the other resonant peaks which originates in $\chi''_{+-}(q=\pi,\omega)$. The second is also common with the other *bulk* resonant peaks. However, resonant peaks involved with the BBS generally depends on the concentration. For instance, let us consider a two-particle intermediate state $|\theta_1,\theta_2\rangle_{B_1B_1}$ in $G^{(1)}_{S^+S^-}(q=\pi,i\omega)$ instead of the one-particle state $|\theta_1\rangle_{B_1}$ in (38). The corresponding term in $G^{(1)}_{S^+S^-}(q=\pi,i\omega)$ is

$$
\begin{aligned}
&\frac{1}{N}{C_s^{\perp}}^2\int_0^\infty d\tau\int_{-\infty}^0 drdX e^{i\omega\tau}\frac{1}{2}\int_{-\infty}^\infty\frac{d\theta}{2\pi}K^{B_1B_1}(\theta)\frac{1}{2}\int_{-\infty}^\infty\frac{d\theta_1 d\theta_2}{(2\pi)^2}\\
&\qquad\qquad\times\langle\mathrm{vac}|e^{-i2\pi R\tilde{\phi}(x_1,\tau)}|\theta_1,\theta_2\rangle_{B_1B_1}{}^{B_1B_1}\langle\theta_2,\theta_1|e^{i2\pi R\tilde{\phi}(x_2,0)}|-\theta,\theta\rangle_{B_1B_1}.
\end{aligned}
$$

Here we assumed $x_1<x_2$ for simplicity. This process leads to a resonant peak in $\chi''_{\mathrm{phys}}(q=0,\omega)$ as follows.

$$\frac{1}{N}\left(\frac{D_z}{J}\right)^2\frac{\pi v{C_s^{\perp}}^2 f_{B_1}F^{-i2\pi R\tilde{\phi}}_{B_1B_1}(-iu_{B_1B_1})F^{i2\pi R\tilde{\phi}}_{B_1B_1}(-iu_{B_1B_1}+i\pi)}{2M_1^2\sin(\pi\xi/2)}\delta(\omega-M_1-M_{\mathrm{BBS}}) \qquad (42)$$

The two-particle form factor $F^{e^{i2\pi R\tilde{\phi}}}_{B_1B_1}(\theta_1-\theta_2)\equiv\langle\mathrm{vac}|e^{i2\pi R\tilde{\phi}(0,0)}|\theta_1,\theta_2\rangle_{B_1B_1}$ is positive when $\theta_1-\theta_2=-iu_{B_1B_1},-iu_{B_1B_1}+i\pi$ [4]. Note that the intensity is proportional to the concentration of non-magnetic impurities because of the factor $1/N$.

The resonance frequency $\omega=M_1+M_{\mathrm{BBS}}$ is a simple superposition of two resonances $\omega=M_1$ and $\omega=M_{\mathrm{BBS}}$. If we consider $G^{(2)}_{S^+S^-}(q=\pi,i\omega)$, we will obtain multi-BBS resonances such as $\omega=2M_{\mathrm{BBS}},M_n+2M_{\mathrm{BBS}}$.

Transverse uniform component $G_{S^+S^-}(q=0,i\omega)$

Below we point out that some boundary resonances cannot be understood by any superposition of the existing resonance frequencies. This new resonance appears in $\chi''_{+-}(q=0,\omega)$. When we are concerned with $q\approx 0$ component of correlation function $G_{S^+S^-}(q,i\omega)$, we may replace

$$S_x^+ \sim \frac{C_u^\perp}{2}\big[\mathcal{O}_S e^{-iHx}+\mathcal{O}_S^\dagger e^{iHx}\big]. \tag{43}$$

The fields $\mathcal{O}_S = e^{-i(2\pi R\tilde{\phi}+\phi/R)}$ and $\mathcal{O}_S^\dagger = e^{i(2\pi R\tilde{\phi}+\phi/R)}$ can create n solitons, m antisolitons and l breathers with $n-m=1$ and $n-m=-1$ respectively. Here l can be arbitrary. Thus, minimal intermediate states in $G_{S^+S^-}(q=0,i\omega)$ are a one-soliton state $|\theta_1\rangle_S$ and a one-antisoliton state $|\theta_1\rangle_{\bar{S}}$.

The uniform component $\chi''_{+-}(q=0,\omega)$ does not lead to the resonance at $\omega=M_{\mathrm{BBS}}$. This is because a "shift of the wavenumber" is accompanied with $\chi''_{+-}(q=0,\omega)$. The bulk soliton resonance occurs at $\omega=E_S=\sqrt{M^2+H^2}$, not at $\omega=M$. E_S is obtained by substituting $q=\pm H$ into the Lorentz invariant dispersion relation $E(q)=\sqrt{M^2+q^2}$ of the soliton. On the other hand, the BBS does not have q-dependent dispersion. Thus, the resonance $\omega=M_{\mathrm{BBS}}$ cannot originate in $\chi''_{+-}(q=0,\omega)$.

An interesting resonance appears in processes involved with multi-particle intermediate states. Let us consider a case in which a two-particle state $|\theta_1,\theta_2\rangle_{B_1S}$ appears as an intermediate state.

$$\begin{aligned}
&\frac{1}{N}\frac{{C_u^\perp}^2}{4}\int_0^\infty d\tau\int_{-\infty}^0 drdX\,e^{i\omega\tau}\frac{1}{2}\sum_{a,b}\int_{-\infty}^\infty\frac{d\theta}{2\pi}K^{ab}(\theta)\int_{-\infty}^\infty\frac{d\theta_1 d\theta_2}{(2\pi)^2}\\
&\qquad\times\Big[\theta_H(x_2-x_1)e^{-iHr}\langle\mathrm{vac}|\mathcal{O}_S(x_1,\tau)|\theta_1,\theta_2\rangle_{B_1S}\,{}^{SB_1}\langle\theta_2,\theta_1|\mathcal{O}_S^\dagger(x_2,0)|-\theta,\theta\rangle_{ab}\\
&\qquad\qquad+\theta_H(x_1-x_2)e^{-iHr}\langle\mathrm{vac}|\mathcal{O}_S(x_2,0)|\theta_1,\theta_2\rangle_{B_1S}\,{}^{SB_1}\langle\theta_2,\theta_1|\mathcal{O}_S^\dagger(x_1,\tau)|-\theta,\theta\rangle_{ab}\Big]
\end{aligned}$$

Both B_1 and S in the intermediate state $|\theta_1,\theta_2\rangle_{B_1S}$ can form the BBS. When the first breather B_1 forms a BBS, the resultant resonance frequency is

$$\omega = M\cosh\theta_0 + M\sin u_{SS}.$$

Since, $M\cosh\theta_0=\sqrt{M^2+H^2}=E_S$ and $M\sin u_{SS}=M_{\mathrm{BBS}}$, this resonance frequency is equal to

$$\omega = E_S + M_{\mathrm{BBS}}. \tag{44}$$

This is a simple superposition of the bulk resonance $\omega=E_S$ and the boundary resonance $\omega=M_{\mathrm{BBS}}$ On the other hand, when the soliton S forms a BBS, the resultant resonance frequency is somewhat strange, which is

$$\omega = E_1 + M_{\mathrm{BBS}}. \tag{45}$$

The first term is given by

$$E_1=\sqrt{M_1^2+H^2}.$$

This resonance frequency (45) cannot be represented by any superposition of existing resonance frequencies. Since a soliton S is trapped at the boundary and transformed into a BBS, a first breather B_1 propagates in the bulk as if it were a soliton.

INTENSITIES OF "UNKNOWN PEAKS"

In our paper, we identified the "unknown modes" found in recent experiments on $KCuGaF_6$ [5] and Cu-PM [6, 7] with the boundary resonances. Here we briefly comment with intensities of the "unknown peaks". The compound $KCuGaF_6$ has larger staggered field ($c_s=0.18$ for $H\parallel c$) than Cu-PM ($c_s=0.083$). Thus, in Cu-PM, intensities of the staggered susceptibilities $\chi''_{+-}(q=\pi,\omega)$ and $\chi''_{zz}(q=\pi,\omega)$ are strongly suppressed because the strength of the staggered DM interaction is equal to $c_s\ll 1$ at most. We may expect that, if boundary resonances exist, they are likely to come from the uniform susceptibility $\chi''_{+-}(q=0,\omega)$. In fact, our assignments of the "unknown modes" in Cu-PM, which are $\omega=E_{B_2}, E_{B_1}+M_1-M_{\mathrm{BBS}}$, are consistent with this speculation. One can find that the breather resonances $\omega=M_n$ are weaker than the "unknown mode" U_1 in Ref. 6. We assigned U_1 to $\omega=E_{B_2}$. While it looks counterintuitive that the boundary mode has the stronger absorption intensities than those of bulk modes, this relation can be understood by the weak mixing of the staggered susceptibilities in (15). The breather resonances come from the staggered part.

$KCuGaF_6$ has relatively stronger staggered field. Ref. 5 shows that the breather resonances at $\omega=M_n$

have approximately the same intensities as the soliton resonances $\omega = E_S$. This experimental observation is also consistent with (15) and the large c_s. As for the "unknown modes", our assignments are consistent with the estimation of the large c_s. We assigned "unknown modes" to $\omega = M_{\mathrm{BBS}}, M_1 + M_{\mathrm{BBS}}, 2M_1 - M_{\mathrm{BBS}}, M_2 - M_1 + M_{\mathrm{BBS}}$, all of which originate in the transverse part $\chi''_{+-}(q = \pi, \omega)$.

[1] I. Affleck and M. Oshikawa, Phys. Rev. B **60**, 1038 (1999).
[2] S. Ghoshal and A. Zamolodchikov, Int. J. Mod. Phys. A **9**, 3841 (1994).
[3] S. Ghoshal, Int. J. Mod. Phys. A **9**, 4801 (1994).
[4] I. Kuzmenko and F. H. L. Essler, Phys. Rev. B **79**, 024402 (2009).
[5] I. Umegaki, H. Tanaka, T. Ono, H. Uekusa, and H. Nojiri, Phys. Rev. B **79**, 184401 (2009).
[6] S. A. Zvyagin, A. K. Kolezhuk, J. Krzystek, and R. Feyerherm, Phys. Rev. Lett. **93**, 027201 (2004).
[7] S. A. Zvyagin, E. Čižmár, M. Ozerov, J. Wosnitza, R. Feyerherm, S. R. Manmana, and F. Mila, Phys. Rev. B **83**, 060409 (2011).